Strong Converse Magneto-Electric Effect in a Composite of Weakly Ferromagnetic Iron Borate and Ferroelectric Lead Zirconate Titanate

M. Popov,[1,2] Y. Liu,[1,3] V. L. Safonov,[4] I. V. Zavislyak,[2] V. Moiseienko,[1,2] P. Zhou,[3] Jiayu Fu,[1,5] Wei Zhang,[1] Jitao Zhang,[6] Y. Qi,[3] Tianjin Zhang,[3] T. Zhou,[5] P. J. Shah,[4] M. E. McConney,[4] M.R. Page,[4] and G. Srinivasan[1 a)]

[1] *Physics Department, Oakland University, Rochester, MI 48309, USA*

[2] *Faculty of Radiophysics, Electronics and Computer Systems, Taras Shevchenko National University of Kyiv, Kyiv, 01601, Ukraine*

[3] *Materials Science and Engineering, Hubei University, Wuhan 430062, China*

[4] *Materials and Manufacturing Directorate, Air Force Research Laboratory, Wright-Patterson Air Force Base, Dayton, Ohio 45433, USA*

[5] *College of Electronics and Information, Hangzhou Dianzi University, Hangzhou 310018, People's Republic of China*

[6] *College of Electrical and Information Engineering, Zhengzhou University of Light Industry, Zhengzhou 450002, China*

ABSTRACT

This report is on a model and experiment on the nature of mechanical strain mediated converse magneto-electric (CME) effect in a composite of single crystal iron borate, a canted antiferromagnet with a weak ferromagnetic moment, and ferroelectric lead zirconate titanate (PZT). The piezoelectric strain generated in PZT by an electric field *E* manifested as a shift in the quasi-ferromagnetic resonance (FMR) field in iron borate due to strong magneto-elastic interactions. The CME interaction strength determined from the data on field shift in FMR versus *E* was 46-54 MHz·cm/kV at 5.5-6.5 GHz. The strength of CME is comparable to the best reported values for composites of ferrimagnetic oxides and PZT. A model that considers the effect of piezoelectric deformation on magnetic order parameters and magnetic resonance in iron borate is

proposed for the CME effects in the composite and estimated ME coupling coefficients are in good agreement with the data. The *E*-tunability of the high-frequency AFMR mode at ~ 300 GHz is estimated to be on the order of 1.7 MHz kV/cm and is very small compared to the quasi-FMR mode. Composites of iron borate and ferroelectrics are very attractive for use in dual electric field and magnetic field tunable signal processing devices due strong CME interactions and the need for a rather small bias magnetic field compared to traditional ferrimagnetic oxide-based devices.

[a] *email: srinivas@oakland.edu*

1. Introduction

Converse magneto-electric effects in ferromagnetic-ferroelectric composite systems is of significant interest for the development of dual electric and magnetic field tunable microwave devices. An electric field E applied to the ferroelectric phase gives rise to a piezoelectric deformation which when transferred to the ferromagnetic phase produces a change in the magnetic order parameter. Such a magnetic response to E can be studied by ferromagnetic resonance (FMR) under an E-field. The shift in the resonance frequency $\omega_F/2\pi$ (which is equivalent to the shift δH_{0r} in the resonance field H_{0r}) as a function of E is measured to determine the CME coefficient $A_f = \delta(\omega_F/2\pi)/E$. The effect was reported in a variety of ferromagnetic (or ferrimagnetic)-ferroelectric composites, including yttrium iron garnet (YIG), nickel ferrite (NFO), M-type strontium (SrM), barium (BaM) hexagonal ferrites or FeGaB alloys for the magnetic phase and lead zirconate titanate (PZT) or lead magnesium niobite-lead titanate (PMN-PT) for the ferroelectric phase [1-7]. Since the strength of CME is directly proportional to the magnetostriction for the magnetic phase, the A_f - values were rather low and in the range 1-3 MHz·cm/kV for composites with YIG and M-type hexaferrites that are known to have a weak magnetostriction [2]. A much stronger CME effects were reported for composites with NFO or FeGaB alloys [2, 7].

Here we report results of the first studies on CME effects in a composite of iron borate, a canted antiferromagnetic system [8], and ferroelectric PZT. Iron borate, $FeBO_3$, often referred to as a green weak ferromagnet in which the antiferromagnetic ordering is slightly canted by the Dzyaloshinskii-Moriya interaction [9-13] with a Neel temperature of 348 K [14, 15]. It has a rhombohedral crystal structure (see Fig. 1a) with its magnetic moments aligned in the (111) plane. The net ferromagnetic moment is small, on the order of $4\pi M \sim 115$ G at 300 K, and magnetic anisotropy fields less than 1 Oe in the easy (111) plane and 62.5 kOe along the hard [111] axis [16,17].

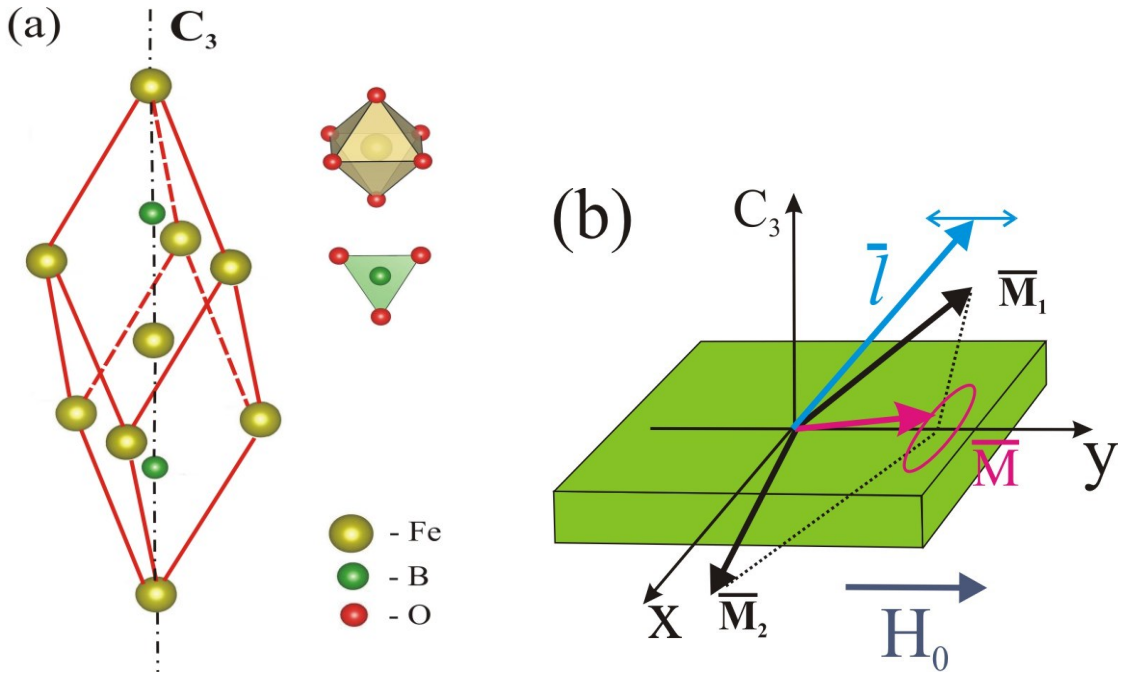

Fig. 1: (a) The rhombohedral unit cell of $FeBO_3$ containing two formula units. Each Fe atom is surrounded by six oxygen, forming an octahedron, and B atoms are situated in the center of flat oxygen equilateral triangle. (b) A sketch showing directions of sublattice magnetizations $\bar{M}_1$, $\bar{M}_2$, weak ferromagnetic moment $\bar{M}$ and antiferromagnetic vector $\bar{l}$. *Also the behavior of $\bar{M}$* and $\bar{l}$ *during quasi-FMR oscillations is schematically shown.*

Studies of $FeBO_3$ reported a low-frequency quasi-FMR mode at frequencies from 5 GHz to 30 GHz for applied fields of a few Oe to a few hundred Oe, and the high-frequency quasi-antiferromagnetic resonance (AFMR) occurs at several hundred GHz [10,11,18,19]. Iron borate was also reported to show very high Faraday rotation at 525 nm [20]. $FeBO_3$ is of interest for studies on parametric excitation of spin waves and magnetoelastic waves [21, 22] and for a variety of applications including magnetic sensors, microwave devices and optical filters and modulators [14, 15, 20].

This study is on (i) theory for the effects of an in-plane strain on the quasi-FMR mode in a single crystal platelet of (111) $FeBO_3$ and the CME effects in a composite with PZT and (ii)

experiments on the nature of CME effects in the composite. In the model we estimated the variation in the magneto-elastic anisotropy field of iron borate due to the in-plane component of the piezoelectric deformation in PZT and the resulting variation in the FMR field or frequency. Expressions for the CME coefficient A were obtained in terms of both field and frequency shift in FMR. This is followed by details on studies on FMR in the composite with a c-plane iron borate and PZT. Measurements in the frequency rage 5 to 7 GHz were carried out and data on the shift in the resonance field as a function of the DC voltage applied to PZT were utilized to estimate the CME coefficient A. Estimated CME coefficients were found to be in good agreement with the data. Details on the model and experiments on the CME effects are provided next.

2. Theoretical background

First, we develop a model for the CME effects in a composite of platelets of iron borate and PZT. It is assumed that PZT is poled perpendicular to its plane and subjected to an electric field along the poling direction and resulting in an in-plane uniaxial piezoelectric deformation that is transmitted to iron borate. In this section we estimate the shift in the resonance field or frequency due to the mechanical deformation and the CME coefficient. There are two uniform magnetic oscillations in $FeBO_3$; a quasi-FMR and a quasi- AFMR modes [8, 23-25]. The quasi-FMR mode frequency can be written as

$$\omega_F/(2\pi) = \gamma\{(H_0+4\pi M(N_x-N_z))\,(H_0+4\pi M(N_y-N_z)+H_{DM})+2H_{\Delta 1}^2+2H_{A1}(V)H_E\}^{1/2} \quad (1a)$$

and approximate expression for the quasi-AFMR mode frequency is

$$\omega_{AF}/(2\pi) = \gamma\{2H_AH_E+H_{DM}(H_0+H_{DM})+H_{\Delta 1}^2+H_{\Delta 2}^2+(H_{A1}(V)+H_{A2}(V))H_E\}^{1/2} \quad (1b)$$

where $\gamma = 2.8$ GHz/kOe is the gyromagnetic ratio, H_0 is the external magnetic field, $4\pi M$ is the net ferromagnetic moment, N_i are the demagnetizing factors, H_{DM} is the Dzyaloshinskii-Moriya field and H_A is an easy-plane anisotropy field. The last terms in Eq. (1) represent the energy gap that is

a function of the exchange field and the magneto-elastic anisotropy field. Specifically, $H_{\Delta 1}^2$ and $H_{\Delta 2}^2$ are the magneto-elastic energy gaps determined by the spontaneous striction (see ref.[23] for exact expressions) and other types of static mechanical deformation, for example, due to defects generated during crystal growth or hydrostatic pressure [23, 26]; $H_{A1}(V)$ and $H_{A2}(V)$ are parts of anisotropy field induced by mechanical stress caused by external forces; and H_E is the exchange field. Due to the large value of H_E any small change in the anisotropy field H_{A1} will have very significant influence on the resonance frequency. In a composite with PZT one expects a variation in $H_{A1}(V)$ for $FeBO_3$ due to the piezoelectric deformation of the PZT under a DC voltage V and, therefore, an electric filed control of the quasi-FMR frequency, according to Eq.(1a).

The expression for H_{A1} in the case of uniaxial deformation in the crystal basal plane is given by [23, 25]

$$H_{A1} = -K\sigma\cos(2\Psi) \tag{2}$$

where σ is the internal uniaxial stress and Ψ is the angle between the deformation direction and the antiferromagnetic vector $\bar{l}$ ($\bar{l}$ is orthogonal to the direction of applied magnetic field $\bar{H}_0$) in the basal plane (see Fig. 1b). The coefficient K is given by

$$K = \frac{1}{4M_0}\frac{(4B_3c_{44} - B_4c_{14})}{2(c_{11} - c_{12})c_{44} - c_{14}^2} \tag{3}$$

where M_0 is the sublattice magnetization, B_i are the magnetoelastic constants, and c_{ij} are the elastic constants. From Eq.(1b), neglecting H_0 and $4\pi M$ in comparison with H_{DM}, and for a fixed resonance frequency, one obtains the following expression for the deformation induced shift of resonance field

$$\delta H_{0r}(V) = (2H_E/H_{DM})K\sigma\cos(2\Psi). \tag{4}$$

In order to compare experimental results with theoretical estimation one needs to determine uniaxial stress acting on the magnetic material. Expressions for this internal stress for the given

in-plane strain (assuming that the planar deformations of PZT and ferrite material are identical) are presented, for example, in Refs. [27, 28]:

$$\sigma_{xx} = \frac{Y}{1-\nu^2}(\varepsilon_{xx} + \nu\varepsilon_{yy}), \sigma_{yy} = \frac{Y}{1-\nu^2}(\varepsilon_{yy} + \nu\varepsilon_{xx}) \tag{5}$$

where Y is magnetic material Young's modulus, ν is the Poisson's ratio, and ε_{ij} is the in-plane strain. Hence, the net uniaxial stress is given by

$$\sigma = \sigma_{xx} - \sigma_{yy} = \frac{Y}{1+\nu}(\varepsilon_{xx} - \varepsilon_{yy}) . \tag{6}$$

In general, both ε_{xx} and ε_{yy} are the functions of transversal coordinates (x,y) and the sample aspect ratio. These functions can be found by solving full electromechanical problem with the proper boundary conditions which is a separate cumbersome task [29]. For the rectangle sample considered in this tudy, in general case, $\varepsilon_{xx} \neq \varepsilon_{yy}$ and some net uniaxial stress along the larger side is always present [29]. We may estimate the maximum stress in the center of the PZT (where $FeBO_3$ sample is situated) by assuming a fundamental transverse deformation mode [30] for which in center $\varepsilon_{xx} >> \varepsilon_{yy}$. Then, neglecting ε_{yy} we obtain

$$\sigma = \frac{Y}{1+\nu}\varepsilon_{xx} = \frac{Y}{1+\nu} d_{31} E , \tag{7}$$

where d_{31} is the piezoelectric coefficient and E is the electric field strength inside the piezoelectric. In summary, the deformation-induced shift of resonance field is

$$\delta H_{0r} = AE \tag{8}$$

where CME coefficient A is given by

$$A = \frac{2H_E}{H_{DM}} K \frac{Y}{1+\nu} d_{31} \cos(2\Psi) \tag{9}$$

Note that the field dependence of the frequency in Eq.(1a) differs from typical FMR frequency and therefore the shift $\delta(\omega_F/2\pi)$ in this frequency is no longer equivalent to the shift

δH_{0r} in the resonance field as it takes place in ferromagnets. The CME coefficient in terms of frequency A_f for iron borate and PZT composite can be calculated using resonance condition (1a):

$$\delta(\omega_F / 2\pi) = \left.\frac{\partial(\omega_F / 2\pi)}{\partial H_0}\right|_{\substack{H_0=H_{0r} \\ H_A=0}} \delta H_{0r} \tag{10}$$

where $\left.\frac{\partial(\omega_F / 2\pi)}{\partial H_0}\right|_{\substack{H_0=H_{0r} \\ H_A=0}} = \frac{\gamma^2 H_{DM}}{2(\omega_F / 2\pi)}$. Taking into account Eqs.(8) and (9) one obtains

$$\delta(\omega_F /2\pi) = -A_f E \tag{11}$$

where

$$A_f = \frac{\gamma^2 H_E}{(\omega_F / 2\pi)} K \frac{Y}{1+\nu} d_{31} \cos(2\Psi) \tag{12}$$

The field and frequency CME coefficients are related by

$$A_f = \frac{\gamma^2 H_{DM}}{2(\omega_F / 2\pi)} A \tag{13}$$

The expressions for the CME coefficients are used in the following section to estimate the ME coefficients for comparison with results from experiments.

Besides the magnetoelastic effect, considered here, the mechanical deformation is also known to result in deformation of the M-O-M bond angles and lengths, which, in turn affects the magnitudes of exchange coupling constants and Dzyaloshinskii–Moriya (DM) interactions [31, 32]. However, it follows from the theory discussed in Refs.31 and 32, a significant change in exchange coupling strengths and DM interactions are expected only for in-plane tensile/compressive strains on the order of 3-4 %. In this study (as discussed in the following section) the strain $\varepsilon \approx d_{31}E$ does not exceed 0.02 % and is expected to lead to a very small variations in H_E and H_{DM} and, therefore, will lead to negligible changes in the resonance magnetic

field. Therefore, we must conclude that although the deformation of the M-O-M bond angles and lengths may be present in $FeBO_3$, their influence on FMR resonance field/frequency, is too weak, and major contribution arises from the magneto-elastic spin-orbital term in Eq. (1).

3. Experimental results and discussion

Flux grown $FeBO_3$ single crystals used in this study were provided by the group at the Taurida National University, Simferopol, Crimea [18]. The *solution in the melt* technique was utilized for the growth to obtain (111) single crystal platelets 0.05 – 0.1 mm in thickness. The bilayer of $FeBO_3$ and PZT, shown in the Fig. 2a, was made by bonding 2 mm × 2 mm × 0.2 mm (111) platelet of iron borate to 10 mm × 5 mm × 0.3 mm polycrystalline PZT (#850 – American Piezo Ceramics [33]). A quick dry epoxy, cyanoacrylate, of thickness 2 μm was used for bonding.

Studies on the CME effect in the iron borate-PZT composite were carried out in two steps. First, profiles of FMR absorption versus magnetic bias field H_0 were obtained for a series of frequencies and the data on resonance magnetic field H_{0r} vs. $\omega_F/(2\pi)$ were used to estimate the magnetic parameters of $FeBO_3$. Second, the resonance profiles were acquired at a constant frequency as a function of DC voltage V applied across the thickness of PZT and data on H_{0r} vs. V were then used to estimate the strength of CME effect.

The broadband FMR measurement setup is shown in Fig. 2b. The sample was placed in a coplanar waveguide excitation structure. A static magnetic field was applied parallel to the sample plane perpendicularly to the larger side of the PZT and perpendicular to the rf magnetic field. A modulating field of amplitude 1 Oe at 1 kHz was applied so that the derivative of the power absorbed P of the sample, dP/dH_0, could be recorded as H_0 was scanned.

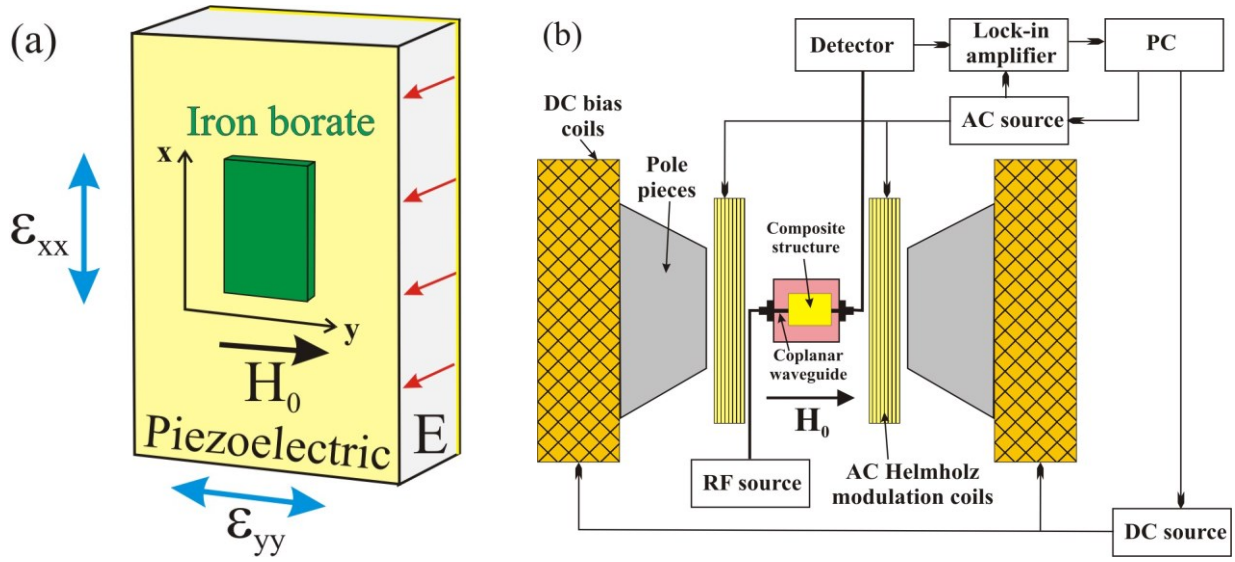

Fig.2: (a) The $FeBO_3$–PZT bilayer composite structure. (b) Block diagram showing the field sweep wideband ferromagnetic resonance measurement system.

Figure 3a shows profiles of dP/dH_0 vs. H_0 at 5.5–7 GHz. The profiles indicate H_{0r} increasing from 31 Oe at 5.5 GHz to 75 Oe at 7 GHz. We did not observe any variation in H_{0r} with the in-plane orientation of magnetic field and any variation would be too small to measure since the in-plane anisotropy field is quite small. The peak-to-peak linewidth ΔH is found to increase with frequency, from ~ 20 Oe at 5.5 GHz to ~ 30 Oe at 7 GHz.

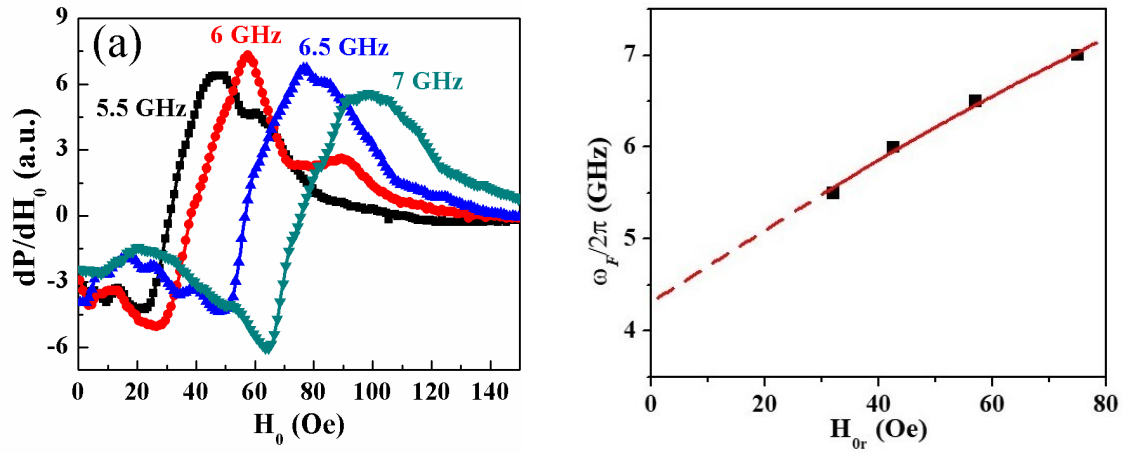

Fig.3: (a) Profiles showing low-frequency quasi-FMR for $FeBO_3$ in a composite with PZT. The inset shows the bilayer composite. (b) Frequency versus resonance field H_{0r} for FMR in the composite. The solid and dashed lines are the theoretical fit to the data.

The data in Fig.3b were used to estimate the magnetic parameters of $FeBO_3$. From the resonance condition in Eq. (1a), neglecting contribution from demagnetizing field and assuming that voltage-induced magneto-elastic field is absent, we get

$$\omega_F/(2\pi) = \gamma\,[H_{0r}\,(H_{0r} + H_{DM}) + 2H_{\Delta l}^{2}]^{1/2}\,. \qquad (14)$$

The resonance frequencies $\omega_F/(2\pi)$ versus H_{0r} were fitted to Eq.(14). The parameters obtained for the FMR data are H_{DM} = 58.8 kOe and $H_{\Delta 1}$=0.99 kOe. These parameters agree with H_{DM} = 62-64 kOe and $H_{\Delta 1}$=1.07 kOe reported in Ref. 11.

Next we focus on the magneto-electric effect. The CME effect in the composite was investigated by FMR at a constant frequency under a static electric field E applied across the PZT layer. Results of measurements at 5.5 GHz are shown in Fig.4. A DC voltage of positive polarity up to a maximum of 350 V was applied. Positive voltage corresponds to same polarity as for the voltage applied for poling the PZT. Representative resonance profiles in Fig.4(a) show a decrease in H_{0r} with the magnitude of voltage. Figure 4(b) shows measured H_{0r} as a function of V. A sharp decrease in H_{0r} from 31 Oe to 18 Oe is measured as V is increased from 0 V to +350 V. The overall V-induced change in H_{0r} is on the order of 13 Oe and, from the data in Fig. 3(b), is equivalent to tuning the quasi-FMR frequency by ~ 500 MHz or 10% tuning of the resonance frequency.

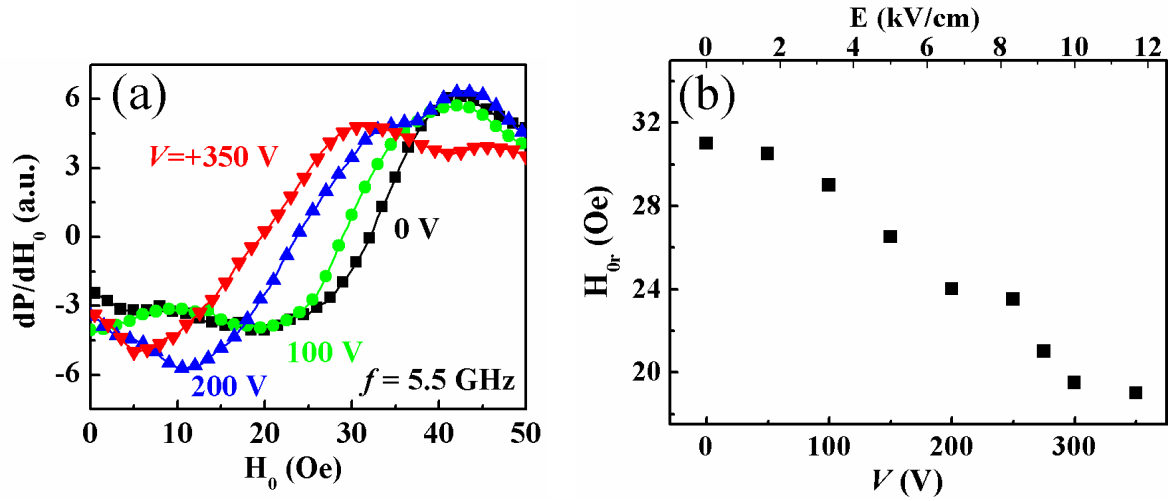

Fig.4. (a) Low-frequency quasi-FMR profiles for $FeBO_3$-PZT composite at 5.5 GHz for DC voltages applied to PZT. (b) Variation of the resonance field H_{0r} as a function V obtained from the profiles as shown in (a).

We consider the cause of CME effects in the composite. First of all, there is a finite deformation in the equilibrium state of the weak ferromagnet, which manifests as a change in the term $H_{\Delta 1}^2$ in Eq.(1a). The *E*-induced FMR frequency/field shift in the $FeBO_3$-PZT system is due to strain mediated ME coupling in the composite. Under an applied *V*, the in-plane component of piezoelectric strain in the PZT layer used in this study is on the order of -175 pm/V. This strain when transferred to iron borate will give rise to an addition to deformation. It will result in an increase in the anisotropy field, which will be a function of the elastic and magneto-elastic constants and applied strain as discussed in Sec.2.

Next we estimate the expected variation in the resonance field with *V* using our model. Upon substituting the magnetic, elastic and magnetoelastic parameters of $FeBO_3$ [25, 34] ($c_{11}=44.5\cdot10^{11}$ erg/cm^3, $c_{12}=14.5\cdot10^{11}$ erg/cm^3, $c_{14}=2.0\cdot10^{11}$ erg/cm^3, $c_{44}=9.5\cdot10^{11}$ erg/cm^3, $B_3=2.5\cdot10^6$ erg/cm^3, $B_4=3.7\cdot10^6$ erg/cm^3, $H_E=2.6\cdot10^6$ Oe, $M_0=1056$ G) and $d_{31}=-1.75\cdot10^{-10}$ m/V for PZT [33] into Eqs.(3) and (9) and calculating Young's modulus and Poisson's ratio using the

expression $Y=(c_{11}-c_{12})\cdot(c_{11}+2c_{12})/(c_{11}+c_{12})$ and $\nu=c_{12}/(c_{11}+c_{12})$ we obtained a CME coefficient $A=\delta H_{0r}/E$=1.5 Oe·cm/kV. Thus V= 300 V applied to the 0.3 mm thick PZT and for the case $cos(2\Psi)=1$ the H_{0r} variation should be -15 Oe. Consequently, the frequency CME coefficient is A_f= 65 MHz·cm/kV for $\omega_F/2\pi$=5.5 GHz.

The data in Fig. 4(b) show that the experimental resonance field variation is smaller than the theoretical estimation, amounting to -13 Oe for V=+350 V with the average CME coefficient being A=1.14 Oe·cm/kV. The frequency CME coefficient is then A_f = 54 MHz·cm/kV. The direction of uniaxial stress during experiments was perpendicular to the bias field (i.e. $\Psi=0$), thus providing the most favorable geometry. Therefore, the agreement between data and model is very good and the minor discrepancy could be attributed to the finite aspect ratio of the piezoelectric platelet.

We carried out similar measurements on CME effect for several FMR frequencies. Figure 5 shows results on V dependence of H_{0r} and the estimated variation of δH_{0r} vs. electric field for resonances at 6 GHz and 6.5 GHz and the features are identical to results in Fig. 3 for 5.5 GHz. One obtains A=1.09 Oe·cm/kV, A_f = 47 MHz·cm/kV at 6.0 GHz and A=1.15 Oe·cm/kV, A_f=46 MHz·cm/kV at 6.5 GHz. These results agree with theoretical predictions according to which δH_{0r} is independent of FMR frequency. The theoretical dependence was obtained using the expression $\delta H_{0r}=-A\cdot E$ with CME coefficient A that has been calculated in the previous section. One can see a reasonable agreement between theory and with the theory predicting a larger change in δH_{0r} with E slope and could be due to the assumption of uniaxial strain $\varepsilon_{xx} >> \varepsilon_{yy}$ assumed in deriving Eq. (7). Data in Figs. 5 were approximated by a linear dependence of δH_{0r} on V. A nonlinear behavior becomes evident for voltage V>300 V due to a switch in the polarization direction in PZT that occurs for E higher than a critical field $E_c \sim$ 11.7 kV/cm in PZT [35].

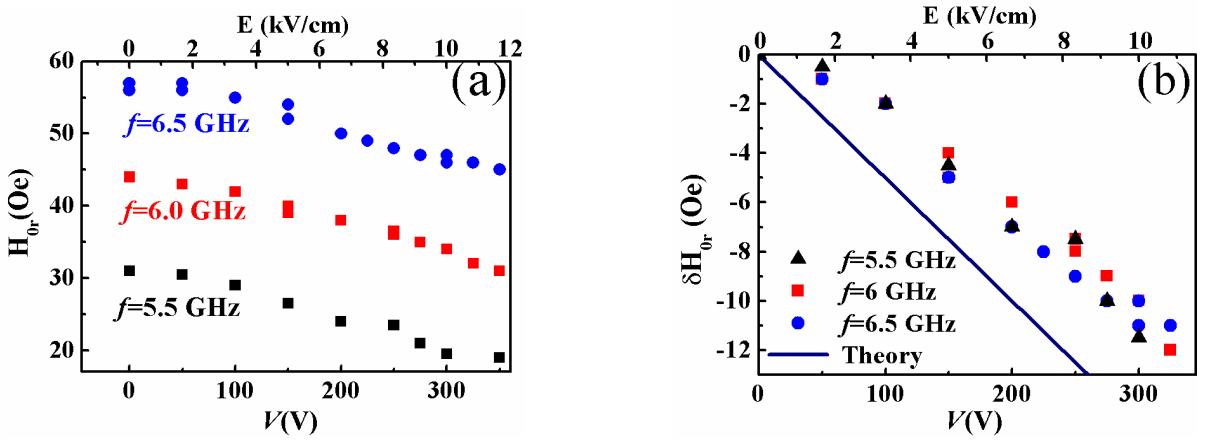

Fig.5: Data on variation in the quasi-FMR resonance field H_{0r} and its experimental and theoretical variations with V for frequencies 5.5 GHz, 6 GHz and 6.5 GHz.

The frequency CME coefficient A_f obtained in this work is compared with reported results for ferrite-ferroelectric composites published elsewhere is presented in the Table 1. The coefficient A_f for $FeBO_3$-PZT is about an order of magnitude higher than those for YIG and M-type hexaferrites [5, 6, 36] and is comparable to A_f= 8 - 50 MHz·cm/kV [37-39] reported for nickel ferrite films prepared by a variety of techniques such as liquid phase epitaxy, pulsed laser deposition and chemical vapor deposition techniques which were used in composites with PMN-PT or PZT. The much higher CME coefficient for iron borate is determined by the specific form of dispersion Eq. (1a) for the quasi-FMR mode, which contains the $2H_EH_A$ term. Due to the presence of a very large H_E prefactor even a small change in the anisotropy field H_A will result in significant changes in the resonance frequency or resonance field. The CME effect for the iron borate and ferroelectric composite could be further strengthened with the use of PMN-PT with *d*-values an order of magnitude higher than for PZT.

Table 1. Comparison of magnetoelectric coefficients for some ferrite-ferroelectric composites.

CME coefficient A_f	**Composite structure**	**Operating frequency**	**Reference**
1.6-2.5 MHz cm/kV	yttrium iron garnet (YIG) – PZT	f=5 GHz	[5]
2.8-15 MHz cm/kV	YIG – lead magnesium niobate -lead titanate (PMN-PT)	f=9.3 GHz	[36]
0.8 MHz cm/kV	barium ferrite – PZT	f=50 GHz	[6]
50 MHz cm/kV	nickel ferrite (NFO) – PMN-PT	f=6–11 GHz	[37]
Up to 31 MHz cm/kV.	nickel zinc ferrite (NZFO) – PZT	f=7–15 GHz	[38]
8.7-25.1 MHz cm/kV	NFO – PZT	f=8–24 GHz	[39]
46-54 MHz cm/kV	Iron borate –PZT	f=5.5–6.5 GHz	This work

Finally, similar CME studies could be carried out for the high-frequency quasi-AFMR mode in iron borate-ferroelectric composites. We have made a theoretical estimation using Eq. (1b) and magnetic and elastic parameters of iron borate from Ref.[23]. Also it was assumed that coefficient K is the same as was measured experimentally for the low-frequency mode. Thus we calculated a maximum frequency shift of 20 MHz for E = 11.2 kV/cm for the unperturbed AFMR mode frequency $\omega_{AF}/(2\pi) \approx 300$ GHz, which corresponds to $A_f = 1.7$ MHz·cm/kV.

The present study, to our knowledge, constitutes the first report on CME in a canted antiferromagnet and a ferroelectric composite and the composite system is very attractive for dual magnetic field and electric field devices for the following reasons. (i) The quasi-FMR mode in iron borate occurs at a much lower DC bias magnetic field that can be produced with a permanent magnet or a solenoid compared to H_0-values for traditional ferrimagnetic materials such as YIG. For example, at 5.5 GHz the FMR occurs for H_0 = 32 Oe in $FeBO_3$ whereas a bias field of 1275 Oe is required for YIG. (ii) The FMR line-width for $FeBO_3$ is small, 25 Oe at 5.5 GHz, and is

comparable to the best values reported for nickel ferrite or lithium ferrite single crystals or epitaxial films. (iii) The E-tuning is rather high for $FeBO_3$ compared to YIG. The frequency tuning at 5.5 GHz for E= 11.2 kV/cm for iron borate is 500 MHz compared to 22 MHz for YIG. Thus, iron borate-PZT composite has the potential for use in miniature microwave devices in which broad-band tuning could be achieved with a magnetic field and narrow band tuning with an electric field.

The quasi-AFMR mode in $FeBO_3$ has a frequency of hundreds of GHz under the same ultralow H_0 values (≈300 GHz for iron borate) and magneto-electric tuning of such modes proposed in this work could lead to device applications in the sub-THz range.

4. Conclusions

Studies on the nature of strain mediated converse ME effects have been carried out on a composite of single crystal iron borate and polycrystalline PZT. An electric field applied across the thickness of PZT resulted in an in-plane piezoelectric deformation, leading to a change in magneto-elastic anisotropy field in iron borate that is observed as a shift in the quasi-FMR frequency. Data on the E-field shift in FMR has been utilized to determine the CME coupling A_f coefficient in the composite. Measurements in the frequency range 5.5-7 GHz yielded A_f = 46-54 MHz cm/kV, the maximum value attained at 5.5 GHz. A model for the CME coupling in the composite is discussed and the estimated A_f= 65 MHz cm/kV is in good agreement with the measured value. Since the proposed ME tuning mechanism affects both quasi-FMR and quasi-AFMR modes is was suggested to use it for higher frequency mode electrical tuning. A theoretical evaluation of quasi-AFMR mode frequency shift yielded a value of 20 MHz for E = 12 kV/cm at 300 GHz, with the effective A_f= 1.7 MHz·cm/kV. Iron borate-PZT composites due to its low FMR linewidth, a relatively small bias magnetic field and large A-values are very attractive for dual *H*-

and *E*-tunable microwave devices such as resonators and filters, capable of operating in both microwave and sub-THz frequency bands.

Acknowledgments

The research at Oakland University was supported by grants from the National Science Foundation (ECCS-1307714, DMR-1808892). Ying Liu was supported by the Chinese Scholarship Council. The efforts at Hubei University was supported by the National Science Foundation of China (Grant Nos. 51372074, 51472078). JZ was supported by a grant from the Natural Science Foundation of China (NSFC), Grant No. 61979287. The research at AFRL was supported by the Air Force Office of Scientific Research under project number FA9550-15RXCOR198 and a Summer Faculty Fellowship for G.S. V.L.S. is grateful to NRC for a fellowship.

References

1. J. Lou, M. Liu, D. Reed, Y. Ren, and N. X. Sun, *Adv. Mater.* **21**, 4711 (2009).

2. N. X. Sun and G. Srinivasan, *SPIN* **2**, 1240004 (2012).

3. S. Shastry, G. Srinivasan, M. I. Bichurin, V. M. Petrov, and A. S. Tatarenko, *Phys. Rev.* B. **70**, 064416 (2004).

4. N. Li, M. Liu, Z. Zhou, N. X. Sun, D. V. B. Murthy, G. Srinivasan, T. M. Klein, V. M. Petrov, and A. Gupta, *Appl. Phys. Lett.* **99**, 192502 (2011).

5. Y. K. Fetisov and G. Srinivasan, *Appl.Phys.Lett.* **88**, 143503 (2006).

6. G. Srinivasan, I. V. Zavislyak, and A. S. Tatarenko, *Appl. Phys. Lett.* **89**, 152508 (2006).

7. H. Su, X. Tang, H. Zhang, and N. X. Sun, *Appl. Phys. Express* **9**, 077301 (2016).

8. V. I. Ozhogin and V. L. Preobrazhenskii, *Sov. Phys. Usp.* **31**, 713 (1988)

9. G. B. Scott, *J. Phys. D* **7**, 1574 (1974).

10. L. V. Velikov, A. S. Prokhorov, E. G. Rudashevskiy, and V. N. Seleznev, *Sov. Phys. JETP* **39**, 909 (1974).

11. W. Jantz and W. Wettling, *Appl. Phys.* **15**, 399 (1978).

12. I. Dzyaloshinsky, *J. Phys. Chem. Solids* **4**, 241 (1958).

13. T. Moriya, *Phys. Rev.* **120**, 91 (1960).

14. A. J. Kurtzig, R. Wolfe, R. C. LeCraw, and J. W. Nielsen, *Appl. Phys. Lett.* **14**, 350 (1969).

15. R. C. LeCraw, R. Wolfe, and J. W. Nielsen, *Appl. Phys. Lett.* **14**, 352 (1969).

16. R. Diehl, *Solid St. Comm.* **17**, 743 (1975).

17. S. G. Ovchinnikov, V.V. Rudenko, and V. I. Tugarinov, *Phys. Solid State* **52**, 112 (2010).

18. M. A. Popov, I. V. Zavislyak, H. L. Chumak, M. B. Strugatsky, S. V. Yagupov, and G. Srinivasan, *J. Appl. Phys.* **118**, 013903 (2015).

19. K. Seleznyova, M. Strugatsky, S. Yagupov, Y. Mogilenec, A. Drovosekov, N. Kreines, P. Rosa, and J. Kliava, *J. Appl. Phys.* **125**, 223905 (2019).

20. E. A. Turov, *J. Magn. Magn. Mater.* **140**, 1737 (1995).

21. B. Ya. Kotyuzhanskii and L. A. Prozorova, *Sov. Phys. JETP* **56**, 903 (1982).

22. A. V. Andrienko, V. L. Safonov, and H. Yamazaki, *J. Phys. Soc.Japan* **67**, 2893 (1998).

23. A.S. Borovik-Romanov and E. G. Rudashevskii, *Sov. Phys. JETP* **20**, 1407 (1964).

24. L. E. Svistov, V. L. Safonov, and K. R. Khachevatskaya, *JETP* **85**, 307 (1997).

25. G. A. Petrakovskii and A. I. Pankrats, *Physica B+C* **86-88**, 1447 (1977).

26. M. B. Strugatsky and K. M. Skibinsky, *Phys. Sol. State* **57**, 1524 (2015).

27. F. Zighem, D. Faurie, S. Mercone, M. Belmeguenai, and H. Haddadi, *J. Appl. Phys.* **114,** 073902 (2013).

28. M. Liu, O.Obi, Z. Cai, J. Lou, G.Yang, K. S. Ziemer, and N. X. Sun1, J. Appl. Phys. **107**, 073916 (2010).

29. V. I. Karlash, *International Applied Mechanics*, **41**, 709 (2005).

30. C.-H. Huang, and C.-C. Ma, *J. Acoustic. Soc. Am.,* **109,** 2780 (2001).

31. Y. Kota, Y. Yoshimori, H. Imamura, and Tsuyoshi Kimura, *Appl. Phys. Lett.* **110**, 042902 (2017).

32. H. J. Zhao, W. Ren, X. M.Chen, and L. Bellaiche, *J. Phys.: Condens. Matter* **25**, 385604 (2013).

33. Physical and piezoelectric properties of APC materials, https://www.americanpiezo.com/apc-materials/piezoelectric-properties.html

34. S. Speidel, *Appl. Phys. A* **28**, 35 (1982).

35. L. E. Cross, "Ferroelectric ceramics: Tailoring properties for specific applications," Ferroelectric ceramics. Ed. N. Setter (Birkhäuser, Basel, 1993).

36. S. Shastry, G. Srinivasan, M. I. Bichurin, V. M. Petrov, and A. S. Tatarenko, *Phys. Rev. B* **70**, 064416 (2004).

37. Li, Ning, M. Liu, Z. Zhou, N. X. Sun, D. V. B. Murthy, G. Srinivasan, T. M. Klein, V. M. Petrov, and A. Gupta, *Appl. Phys. Lett.* **99**, 192502 (2011).

38. Zhou, Peng, M. A. Popov, Y. Liu, R. Bidthanapally, D. A. Filippov, T. Zhang, Y. Qi et al. *Phys. Rev. Materials* **3**, 044403 (2019).

39. Zhou, Peng, A. V. Singh, Z. Li, M. A. Popov, Y. Liu, D. A. Filippov, T. Zhang et al, *Phys. Rev. Applied* **11**, 054045 (2019).